ACS OMEGA

http://pubs.acs.org/journal/acsodf

Article

Isotherm Modeling and Statistical Physics Interpretation of Dye and Pesticide Adsorption on Activated Carbons for Environmental Remediation

Elham A. Alzahrani, Fatma Dhaouadi,* Lotfi Sellaoui,* Mohamed Bouzidi, Adrián Bonilla-Petriciolet, Nuha Othman S Alsaif, Nawal S. Alshammari, Odeh A. O. Alshammari, and Alessandro Erto

Cite This: https://doi.org/10.1021/acsomega.5c07212

Read Online

ACCESS | Metrics & More | Article Recommendations

ABSTRACT: A multilayer adsorption model was used to explain the adsorption mechanism of two toxic organic pollutants, methylene blue (MB) and 2,4-dichlorophenoxyacetic acid (2,4-D), on a commercial activated carbon (CPAC) and olive stone activated carbon prepared with $ZnCl_2$ ($ZnCl_2$/OSAC). Statistical physics-based modeling showed that the adsorption of both pollutants on tested activated carbons was multimolecular where 2−4 layers can be formed on the adsorbent surface. The calculated saturation adsorption capacities of $ZnCl_2$/OSAC and CPAC for MB were 481−574 and 873−932 mg/g at 30−50 °C, respectively, while the saturation 2,4-D adsorption capacities were 392−607 and 526−675 mg/g for the same adsorbents. Endothermic adsorption was observed for MB, while 2,4-D removal was exothermic. It was found that the MB and 2,4-D removal implied an inclined adsorption geometry, where physical interaction forces contributed to separating these pollutants. Overall, this research provides new findings to explain the adsorption mechanism of these relevant water pollutants on carbonaceous-based materials.

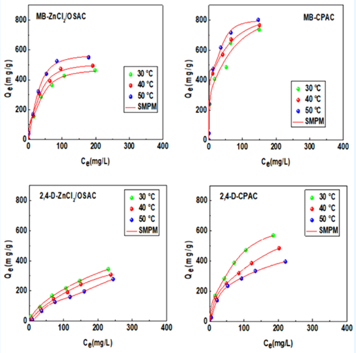

1. INTRODUCTION

The presence of emerging contaminants such as dyes, pesticides, and pharmaceuticals[1−5] in water at trace concentrations is a major problem for human health, and this pollution scenario has generated new technological challenges to satisfy the regulations for environmental protection.[6−8] For instance, current statistics indicate that the herbicides market reached 1.4 million metric tons in the last years.[9] The high consumption of these compounds facilitates their discharge into the environment polluting the water resources.[10,11] Similarly, the dyes are widely used in various industrial sectors (e.g., paper food, pharmaceuticals, and cosmetics)[12−15] generating a relevant problem to depollute their effluents because dye molecules are toxic compounds to the human organism and ecosystems.[16,17] Several studies have focused on mitigating the pollution caused by these compounds with the aim of improving water quality and protecting public health.[18−21]

The selection of the best adsorbent to depollute industrial effluents is a key parameter to handle the environmental impacts caused by the current consumption of dyes and pesticides. A detailed review of the literature indicates that activated carbon is the best commercial multifunctional material for water treatment that contains pesticides, pharmaceuticals, dyes, and heavy metals.[22−32] In this context, methylene blue (MB) is a widely used cationic dye and 2,4-dichlorophenoxyacetic acid (2,4-D) is a common herbicide. These compounds are frequently found in water resources and represent two major classes of emerging organic contaminants to understand the performance and adsorption properties of activated carbon for water depollution.[33−37] Based on these facts, they were selected in this study as model pollutants to analyze their adsorption on an activated carbon surface. Specifically, the present study has focused on the analysis of 2,4-D and MB adsorption on samples of commercial powdered activated carbon (CPAC) and activated carbon prepared from olive stones with $ZnCl_2$ activation ($ZnCl_2$/OSAC). For these adsorption systems, Ozcan et al.[38] applied traditional models to elucidate their removal mechanisms via the analysis of experimental data. However, the theoretical approach used by these authors provided a simple explanation of the adsorption mechanisms for both pollutants, which did not allow us to understand both steric and energetic parameters associated with the separation of these important contaminants.

The present study reports an improved statistical physical model to interpret the adsorption data of 2,4-D and MB using CPAC and $ZnCl_2$/OSAC with the objective of analyzing and understanding their adsorption properties and performance. A

Received: July 22, 2025
Revised: October 14, 2025
Accepted: October 17, 2025

multilayer model with saturation was applied to rationalize the adsorption mechanism of these systems. Consequently, the aim of this paper is to provide an improved vision at the molecular level of the separation of MB and 2,4-D from aqueous solutions using activated carbon surfaces.

2. MB AND 2,4-D ADSORPTION DATA

Figure 1 presents the experimental data for the adsorption of MB and 2,4-D pollutants on CPAC and $ZnCl_2$/OSAC. Adsorption isotherms for these systems were reported by Ozcan et al.[38] Specifically, these authors quantified the adsorption equilibria of both pollutants on tested activated carbons using batch adsorbers operated at 30−50 °C, adsorbent dosage of 0.1 g, contact time of 18 h, and pH 10 for MB and pH 2 for 2,4-D, respectively. Note that both adsorbents showed different textural parameters and surface chemistry as reported in ref 38. These experimental data were used in the present work to perform a theoretical analysis via statistical physics calculations to characterize their adsorption mechanisms.

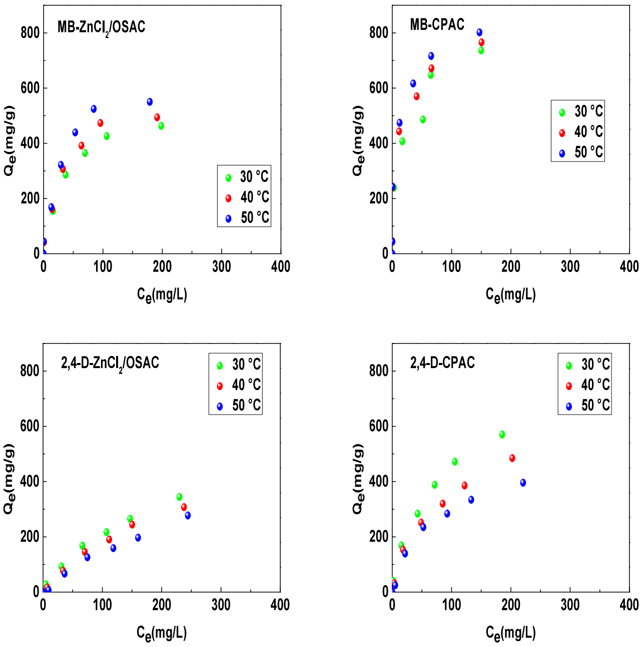

Figure 1. Experimental isotherms reported in ref 38 for the adsorption of MB, and 2,4-D pollutants on $ZnCl_2$/OSAC and CPAC activated carbons.

Experimentally, it was observed that the equilibrium adsorption profiles of MB and 2,4-D pollutants increased with equilibrium concentration in the aqueous solution at tested temperatures until the surface saturation was achieved for both $ZnCl_2$/OSAC and CPAC. This expected plateau indicated that the active sites on the activated carbon surface were fully occupied. The adsorption of these pollutant molecules on the activated carbon surfaces can imply the formation of multiple layers due to their chemical structures. However, the increase in aqueous solution temperature caused a different impact on the adsorption of tested pollutants on $ZnCl_2$/OSAC and CPAC. Specifically, MB removal was endothermic where the adsorption capacities were better at higher temperatures, whereas 2,4-D adsorption was exothermic showing a reduction of its removal as the solution temperature increased, see Figure 1. A statistical physics multilayer model (SMPM) was implemented to elucidate the mechanisms for the adsorption of these organic pollutants on the tested activated carbons. Previous studies[39−41] have demonstrated that SMPM outperformed conventional adsorption models, such as the Langmuir and Freundlich equations, to estimate separation steric parameters for the removal of organic molecules. Herein, it is also convenient to indicate that previous studies based on computational chemistry calculations have shown that molecular aggregation can be expected in aqueous solutions of organic molecules, thus favoring the formation of multilayers on adsorbent surface.[42] Therefore, the characteristics of this multilayer model allow a better understanding of the removal processes of organic adsorbates, providing key parameters for the rationalization of the adsorption mechanisms.

This statistical physics model was formulated based on statistical physics theory, in particular, the grand canonical ensemble considering that the adsorption of pollutant molecules on $ZnCl_2$/OSAC and CPAC surfaces occurs via the formation of a variable number of adsorbate layers where two interaction energies are present. The first energy parameter ($-\varepsilon_1$) describes the interactions between the adsorbed pollutant molecules and the activated carbon surface (i.e., pollutant−activated carbon interactions). This parameter governs the initial separation stage of the pollutant and controls the stability of the primary adsorption layer. The second energy parameter ($-\varepsilon_2$) is associated with the interactions involved in the molecular aggregates that are responsible for the formation of subsequent adsorbate layers (i.e., molecule−molecule interactions). The balance between ($-\varepsilon_1$) and ($-\varepsilon_2$) therefore determines the extent of multilayer adsorption and the overall configuration of the adsorbed phase. Consequently, the total number of layers formed is expressed as $1 + N_2$ where N_2 is the number of layers formed via the second energy interaction (i.e., molecular aggregates). If $1 + N_2 \approx 1$, the adsorption process approaches a monolayer process, whereas $1 + N_2 \approx 2$ indicates the formation of a double layer structure.

The mathematical expression of SMPM for analyzing the pollutant adsorption on activated carbons is presented by the following equation:[39,43]

$$Q_e = n_{pm} D_{aas} \frac{\dfrac{-2\left(\frac{C_e}{C_1}\right)^{2n_{pm}}}{1-\left(\frac{C_e}{C_1}\right)^{n_{pm}}} + \dfrac{\left(\frac{C_e}{C_1}\right)^{n_{pm}}\left(1-\left(\frac{C_e}{C_1}\right)^{2n_{pm}}\right)}{\left(1-\left(\frac{C_e}{C_1}\right)^{n_{pm}}\right)^2} + \dfrac{2\left(\frac{C_e}{C_1}\right)^{n_{pm}}\left(\frac{C_e}{C_2}\right)^{n_{pm}}\left(1-\left(\frac{C_e}{C_2}\right)^{n_{pm}N_2}\right)}{\left(1-\left(\frac{C_e}{C_2}\right)^{n_{pm}}\right)} - \dfrac{N_2\left(\frac{C_e}{C_1}\right)^{n_{pm}}\left(\frac{C_e}{C_2}\right)^{n_{pm}}\left(\frac{C_e}{C_2}\right)^{n_{pm}N_2}}{\left(1-\left(\frac{C_e}{C_2}\right)^{n_{pm}}\right)} + \dfrac{\left(\frac{C_e}{C_1}\right)^{n_{pm}}\left(\frac{C_e}{C_2}\right)^{2n_{pm}}\left(1-\left(\frac{C_e}{C_2}\right)^{n_{pm}N_2}\right)}{\left(1-\left(\frac{C_e}{C_2}\right)^{n_{pm}}\right)^2}}{\dfrac{\left(1-\left(\frac{C_e}{C_1}\right)^{2n_{pm}}\right)}{\left(1-\left(\frac{C_e}{C_1}\right)^{n_{pm}}\right)} + \dfrac{\left(\frac{C_e}{C_1}\right)^{n_{pm}}\left(\frac{C_e}{C_2}\right)^{n_{pm}}\left(1-\left(\frac{C_e}{C_2}\right)^{n_{pm}N_2}\right)}{\left(1-\left(\frac{C_e}{C_2}\right)^{n_{pm}}\right)}} \quad (1)$$

This model can be used to calculate key parameters to characterize the adsorption mechanism: the number of pollutant molecules adsorbed per active site on the activated carbon surface (n_{pm}), the density of these active sites (D_{aas}), and two half-saturation concentrations (C_1 and C_2) that are related to the formation of first and consecutive N_2 layers, respectively.

Equation 1 was used to fit all of the experimental isotherms of both pollutants and activated carbons. The results of this model were used to characterize the multilayer nature of tested systems and to determine their steric parameters (n_{pm}, D_{aas}, saturation adsorption capacities) and interaction energies. The experimental data were fitted by using the Levenberg−Marquardt algorithm via a multivariate nonlinear regression. The statistical analysis of model performance was based on the determination coefficient (R^2) besides the identifying of a proper trend in the calculated model parameters versus the adsorption temperature.

https://doi.org/10.1021/acsomega.5c07212
ACS Omega XXXX, XXX, XXX−XXX

Table 1. Calculated SMPM Parameters for MB and 2,4-D Adsorption on CPAC and $ZnCl_2$/OSAC Activated Carbons

T (°C)	Determination coefficient, R^2	Number of molecules adsorbed per active site, n_{pm}	Density of the active sites, D_{aas} (mg/g)	Number of formed layers, $(1+ N_2)$	Concentration at half saturation C_1(mg/L)	Concentration at half saturation C_2(mg/L)	Adsorption capacity at saturation, Q_s (mg/g)
			MB-$ZnCl_2$/OSAC				
30	0.995	1.186	101.992	3.975	1.422	43.220	480.825
40	0.990	1.220	109.387	3.867	1.684	38.420	516.059
50	0.986	1.574	127.286	2.865	8.537	37.266	573.997
			MB-CPAC				
30	0.990	1.249	264.270	2.644	2.125	155.397	872.713
40	0.962	1.200	335.807	2.210	0.365	62.416	890.560
50	0.978	1.025	427.957	2.125	0.655	56.726	932.128
			2,4-D- $ZnCl_2$/OSAC				
30	0.998	0.985	179.375	3.436	35.270	276.492	607.087
40	0.996	1.293	105.803	3.125	35.060	185.525	426.826
50	0.999	2.453	55.946	2.857	37.451	228.485	392.081
			2,4-D-CPAC				
30	0.999	1.042	166.593	3.886	4.807	82.431	674.570
40	0.999	1.397	171.656	2.804	13.464	171.377	671.449
50	0.999	1.664	146.961	2.150	19.059	196.888	525.767

Calculated R^2 values and trends of the steric and energetic parameters indicated that SMPM was the best option for examining MB and 2,4-D adsorption mechanisms at the microscopic scale. This conclusion agreed with previous studies using the same pollutants. For instance, Sboui et al.[40] and Aouaini et al.[44] demonstrated that the adsorption of MB and 2,4-D can involve the formation of a limited number of layers on the surfaces of britholites and a modified biomass. The summary of SMPM parameters for MB and 2,4-D activated carbon systems is reported in Tables 1 and 2, while Figure 2 illustrates the results of SMPM fitting to their experimental isotherms. It is convenient to remark that the other two advanced models were applied in the analysis of adsorption data, i.e.: monolayer model with one energy and double layer model with two energies. The application of these models on tested adsorption data failed because the calculated values for some model parameters were inconsistent with respect to the experiments, besides the impact of temperature on model parameters did not show proper trends.

Table 2. Calculated Interaction Energies for the Adsorption of MB and 2,4-D on $ZnCl_2$/OSAC and CPAC Activated Carbons

T (°C)	$(-\varepsilon_1)$(kJ/mol)	$(-\varepsilon_2)$(kJ/mol)
	MB- $ZnCl_2$/OSAC	
30	25.713	17.144
40	26.196	18.064
50	22.654	18.702
	MB-CPAC	
30	24.705	13.932
40	30.171	16.803
50	29.532	17.576
	2,4-D- $ZnCl_2$/OSAC	
30	7.062	1.893
40	7.331	2.999
50	7.379	2.533
	2,4-D-CPAC	
30	12.068	4.931
40	9.820	3.205
50	9.190	2.932

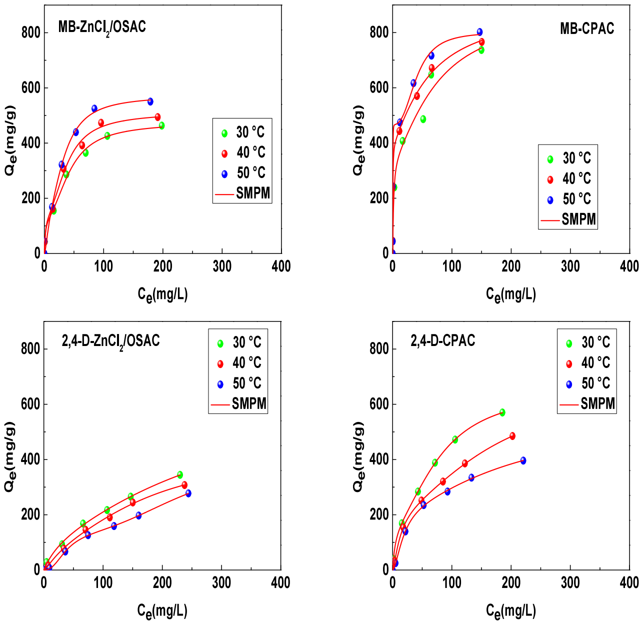

Figure 2. Modeling results using SMPM for the adsorption of MB and 2,4-D molecules on CPAC and $ZnCl_2$/OSAC activated carbons.

3. RESULTS ANDDISCUSSION

3.1. Analysis of the n_{pm}, D_{aas} and N_2 Parameters.

Initially, the adsorption mechanisms of MB and 2,4-D molecules were theoretically characterized via the analysis of parameter $n_{pm,}$ which is defined as a stoichiometric coefficient. This parameter can be used to estimate the degree of molecular aggregation during the adsorption process. Calculated values of this parameter are 1.186, 1.220, and 1.574 for the MB-$ZnCl_2$/OSAC system at 30, 40, and 50 °C, respectively, and 1.249, 1.200, and 1.025 for the MB-CPAC system at the same temperature conditions. For 2,4-D adsorption, the calculated values of n_{pm} were 0.985, 1.293, and 2.453 using $ZnCl_2$/OSAC at 30, 40, and 50 °C, respectively, and 1.042, 1.397, and 1.664 for CPAC at the same operating conditions. Calculated n_{pm} values for these adsorption systems ranged from 1 to 2 indicating that the molecular aggregation of both pollutants was feasible, where dimers and trimers could be formed. On the other hand, $n_{pm} > 1$

indicated that these adsorbates can be removed mainly via an inclined (nonparallel) orientation[39,41,45] of MB and 2,4-D molecules on the investigated activated carbon surfaces. Figure 3 shows the relationship between the aqueous solution temperature and the steric parameter. The increase of the aqueous solution temperature led to higher calculated n_{pm} values for the adsorption of both dye and pesticide molecules on $ZnCl_2$/OSAC. In contrast, the change of the adsorption temperature decreased the calculated n_{pm} values for MB adsorption on CPAC, but it increased the n_{pm} values for the adsorption of 2,4-D molecules. These trends are related to the impact of adsorption temperature on the mass transfer of both pollutants and the role of both adsorbate molecular dimension and textural parameters of activated carbons. Particularly, the microporosity of both adsorbents played a more relevant role during the adsorption of 2,4-D because this pollutant showed a molecular dimension lower than that of MB.

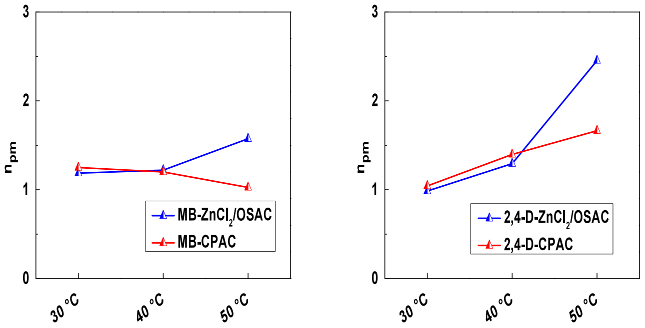

Figure 3. Impact of adsorption temperature on calculated n_{pm} parameter for MB and 2,4-D adsorption on CPAC and $ZnCl_2$/OSAC activated carbons.

The modeling results indicated that the impact of aqueous solution temperature on parameter D_{aas} has also an opposite trend for both pollutants depending on activated carbon used in the removal process, see Figure 4. The opposite trends in D_{aas} arise from differences in surface chemistry and porosity between CPAC and $ZnCl_2$/OSAC, which determine whether the change in separation temperature promotes molecular packing or destabilizes adsorption sites. Also, inverse trends were observed between n_{pm} and D_{aas}. For instance, the n_{pm} parameter increased when the adsorption temperature increased for MB adsorption on $ZnCl_2$/OSAC, while the corresponding adsorption site density decreased.

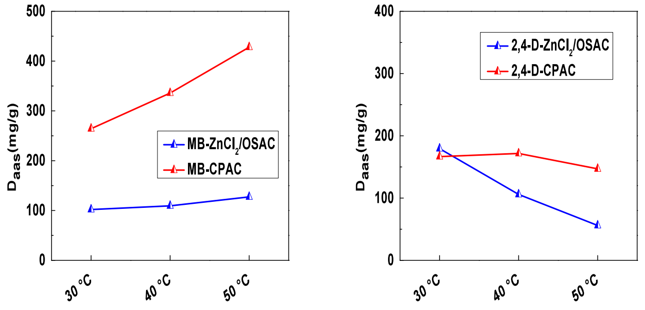

Figure 4. Impact of adsorption temperature on calculated D_{aas} parameter for MB and 2,4-D adsorption on CPAC and $ZnCl_2$/OSAC activated carbons.

SMPM contains a parameter that can be used to estimate the total number of formed layers ($1+N_2$) during the adsorption of MB and 2,4-D pollutants. The calculated values of the N_2 parameter are summarized in Table 1. For the adsorption of MB on $ZnCl_2$/OSAC and CPAC, the values of $1+N_2$ are 3.975, 3.867, and 2.865, and 2.644, 2.210, and 2.125 at 30, 40, and 50 °C, respectively. The analysis of these values indicated that MB was removed via the formation of 2−4 layers on both $ZnCl_2$/OSAC and CPAC surfaces, respectively. Similarly, 2,4-D was adsorbed, forming 2−4 layers on adsorbent surfaces at different temperatures. This difference in the total number of formed layers is probably related to the chemical structures of these compounds (mainly their molecular sizes) and their adsorbent textural properties. The influence of adsorption temperature on the total number of formed layers is described in Figure 5. It was concluded that this operating parameter plays a minor role in layer formation for the removal of both MB and 2,4-D.

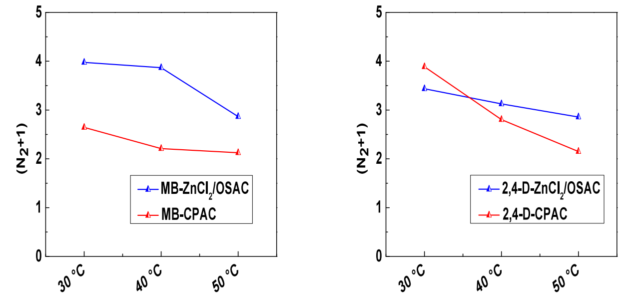

Figure 5. Impact of adsorption temperature on calculated ($1+N_2$) parameter for MB and 2,4-D adsorption on CPAC and $ZnCl_2$/OSAC activated carbons.

3.2. Adsorbent Performance at Saturation Conditions.

MB and 2,4-D adsorption capacities at saturation were determined using the relationship: $n_{pm} \times D_{aas} \times (1+N_2)$. The model calculations indicated that Q_s (MB-CPAC) > Q_s (MB-$ZnCl_2$/OSAC) and Q_s (2,4-D −CPAC) > Q_s (2,4-D - $ZnCl_2$/OSAC) confirming that CPAC was the best adsorbent for the removal of both water pollutants. The performance of CPAC is mainly related to both its textural parameters and its surface chemistry. An analysis of the temperature impact on the saturation adsorption capacities for both MB and 2,4-D pollutants is illustrated in Figure 6. For MB, the separation performance of both activated carbons increased with the increment of the aqueous solution temperature. The improved separation performance for MB at higher temperatures can be

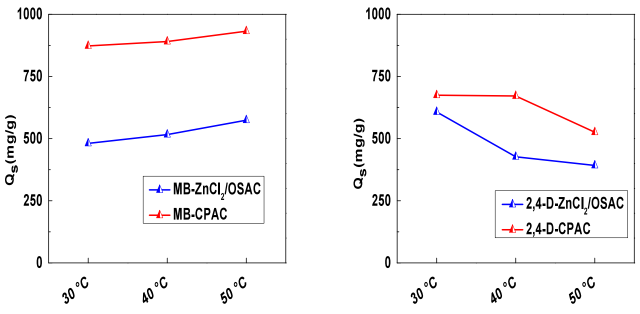

Figure 6. Impact of adsorption temperature on calculated saturation adsorption capacities for MB and 2,4-D adsorption on CPAC and $ZnCl_2$/OSAC activated carbons.

https://doi.org/10.1021/acsomega.5c07212

attributed to the endothermic adsorption process, where enhanced molecular mobility and aggregation favor multilayer formation on the external adsorbent surface. These results confirmed that temperature is a relevant factor in MB removal and that it is convenient to operate at high temperatures to guarantee a better adsorption of this textile pollutant. In contrast, the saturation 2,4-D adsorption capacity decreased with increasing temperature, indicating that the removal of 2,4-D was exothermic and more effective at low temperatures.

3.3. Interaction Energies for MB and 2,4-D Adsorption.

The adsorption energies associated with the removal of MB and 2,4-D molecules by $ZnCl_2$/OSAC and CPAC were determined using the following expressions:[39,43]

$$(-\varepsilon_1) = RT\ln\left(\frac{C_s}{C_1}\right) \quad (2)$$

$$(-\varepsilon_2) = RT\ln\left(\frac{C_s}{C_2}\right) \quad (3)$$

where $R = 8.314$ J mol^{-1} K^{-1} is the ideal gas constant, and C_s is the water solubility of MB and 2,4-D. The calculated adsorption energies for all the tested adsorption systems are presented in Table 2.

All calculated adsorption energies for the tested molecules were <30 kJ/mol, indicating that the removal of both compounds by the two activated carbons was predominantly governed by physical interaction forces. It was proposed that the adsorption mechanism of MB and 2,4-D compounds on $ZnCl_2$/OSAC and CPAC surfaces involves both electrostatic interactions and van der Waals forces.[38] The calculated interaction energies for pollutant molecule−adsorbent surface were higher than those of the molecular aggregates forming the subsequent layers. The relatively low energy values of these molecule−molecule interactions partially explained the decrease in the number of adsorbed molecular layers on the activated carbon surfaces as the temperature of the aqueous solution increased.

CONCLUSIONS

A multilayer adsorption mechanism was involved in the separation of MB and 2,4-D molecules from aqueous solutions using CPAC and $ZnCl_2$/OSAC. Statistical physics calculations revealed that the adsorption process of these compounds primarily followed a multimolecular pathway with the formation of 2−4 layers depending on the system. Overall, the adsorption temperature effects highlight that MB adsorption is endothermic, whereas 2,4-D adsorption is exothermic. The results suggested that the adsorbent microporosity played a relevant role to remove these pollutants due to their different molecular dimensions. In all cases, physical interaction forces were the dominant contributors to the pollutant removal mechanisms. These theoretical results provide valuable insights into the adsorption mechanism at the molecular scale and contribute to a better understanding of the removal of toxic organic pollutants from water using carbonaceous materials.

AUTHOR INFORMATION

Corresponding Authors

Fatma Dhaouadi − *Laboratory of Quantum and Statistical Physics, LR18ES18, Monastir University, Faculty of Sciences of Monastir, Monastir 5000, Tunisia;* orcid.org/0000-0001-9671-7804; Email: dhaouadi.fatma@isimm.u-monastir.tn

Lotfi Sellaoui − *Laboratory of Quantum and Statistical Physics, LR18ES18, Monastir University, Faculty of Sciences of Monastir, Monastir 5000, Tunisia; CRMN, Centre for Research on Microelectronics and Nanotechnology of Sousse, NANOMISENE, 4054 Sousse, Tunisia*; Email: sellaouilotfi@yahoo.fr

Authors

Elham A. Alzahrani − *Department of Chemistry, College of Science, University of Ha'il, Ha'il 81451, Saudi Arabia*

Mohamed Bouzidi − *Department of Physics, College of Science, University of Ha'il, Ha'il 55476, Saudi Arabia*

Adrián Bonilla-Petriciolet − *Tecnológico Nacional de México - Instituto Tecnológico de Aguascalientes, Department of Chemical Engineering, Aguascalientes 20256, Mexico*

Nuha Othman S Alsaif − *Department of Chemistry, College of Science, University of Ha'il, Ha'il 81451, Saudi Arabia*

Nawal S. Alshammari − *Department of Chemistry, College of Science, University of Ha'il, Ha'il 81451, Saudi Arabia*

Odeh A. O. Alshammari − *Department of Chemistry, College of Science, University of Ha'il, Ha'il 81451, Saudi Arabia*

Alessandro Erto − *Dipartimento di Ingegneria Chimica, dei Materiali e della Produzione Industriale, Università degli Studi di Napoli Federico II, 80125 Napoli, Italy;* orcid.org/0000-0002-6956-7924

Complete contact information is available at: https://pubs.acs.org/10.1021/acsomega.5c07212

Notes

The authors declare no competing financial interest.

ACKNOWLEDGMENTS

This research has been funded by Scientific Research Deanship at University of Ha'il − Saudi Arabia through project number RG-24 057.

REFERENCES

(1) Gill, J. P. K.; Sethi, N.; Mohan, A.; Datta, S.; Girdhar, M. Glyphosate Toxicity for Animals. *Environ. Chem. Lett.* **2018**, *16* (2), 401−426.

(2) Al-Salih, M.; Samsudin, S.; Arshad, S. S. Synthesis and Characterizations Iron Oxide Carbon Nanotubes Nanocomposite by Laser Ablation for Anti-Microbial Applications. *J. Genet Eng. Biotechnol* **2021**, *19* (1), 76.

(3) Pereira, H. A.; Hernandes, P. R. T.; Netto, M. S.; Reske, G. D.; Vieceli, V.; Oliveira, L. F. S.; Dotto, G. L. Adsorbents for Glyphosate Removal in Contaminated Waters: A Review. *Environ. Chem. Lett.* **2021**, *19* (2), 1525−1543.

(4) Vargas, V. H.; Paveglio, R. R.; Pauletto, P. de S.; Salau, N. P. G.; Dotto, L. G. Sisal Fiber as an Alternative and Cost-Effective Adsorbent for the Removal of Methylene Blue and Reactive Black 5 Dyes from Aqueous Solutions. *Chem. Eng. Commun.* **2020**, *207* (4), 523−536.

(5) Coldebella, P. F.; Fagundes-Klen, M. R.; Nishi, L.; Valverde, K. C.; Cavalcanti, E. B.; Andreo Dos Santos, O. A.; Bergamasco, R. Potential Effect of Chemical and Thermal Treatment on the Kinetics, Equilibrium, and Thermodynamic Studies for Atrazine Biosorption by the *Moringa Oleifera* Pods. *Can. J. Chem. Eng.* **2017**, *95* (5), 961−973.

(6) Ifebajo, A. O.; Oladipo, A. A.; Gazi, M. Efficient Removal of Tetracycline by CoO/CuFe2O4 Derived from Layered Double Hydroxides. *Environ. Chem. Lett.* **2019**, *17* (1), 487−494.

(7) Ponnuchamy, M.; Kapoor, A.; Senthil Kumar, P.; Vo, D.-V. N.; Balakrishnan, A.; Mariam Jacob, M.; Sivaraman, P. Sustainable Adsorbents for the Removal of Pesticides from Water: A Review. *Environ. Chem. Lett.* **2021**, *19* (3), 2425−2463.

(8) Jiang, X.; Ouyang, Z.; Zhang, Z.; Yang, C.; Li, X.; Dang, Z.; Wu, P. Mechanism of Glyphosate Removal by Biochar Supported Nano-Zero-Valent Iron in Aqueous Solutions. *Colloids Surf. A-Physicochem. Eng. Asp* **2018**, *547*, 64−72.

(9) Food and Agriculture Organization of the United Nations. Pesticides Use, Pesticides Trade and Pesticides Indicators, 2022. See the following: https://openknowledge.fao.org/items/fe5e9454-8c11-4f34-9d00-15746cb2054c (accessed 2024-10-20).

(10) Saleh, I. A.; Zouari, N.; Al-Ghouti, M. A. Removal of Pesticides from Water and Wastewater: Chemical, Physical and Biological Treatment Approaches. *Environ. Technol. Inno.* **2020**, *19*, 101026.

(11) Akash, S.; Sivaprakash, B.; Rajamohan, N.; Pandiyan, C. M.; Vo, D.-V. N. Pesticide Pollutants in the Environment−A Critical Review on Remediation Techniques, Mechanism and Toxicological Impact. *Chemosphere* **2022**, *301*, 134754.

(12) Benhouria, A.; Islam, M. A.; Zaghouane-Boudiaf, H.; Boutahala, M.; Hameed, B. H. Calcium Alginate−Bentonite−Activated Carbon Composite Beads as Highly Effective Adsorbent for Methylene Blue. *Chem. Eng.J.* **2015**, *270*, 621−630.

(13) Li, Y.; Du, Q.; Liu, T.; Sun, J.; Wang, Y.; Wu, S.; Wang, Z.; Xia, Y.; Xia, L. Methylene Blue Adsorption on Graphene Oxide/Calcium Alginate Composites. *Carbohydr. Polym.* **2013**, *95* (1), 501−507.

(14) Ravi; Pandey, L. M. Enhanced Adsorption Capacity of Designed Bentonite and Alginate Beads for the Effective Removal of Methylene Blue. *Appl. Clay. Sci.* **2019**, *169*, 102−111.

(15) Nasrullah, A.; Bhat, A. H.; Naeem, A.; Isa, M. H.; Danish, M. High Surface Area Mesoporous Activated Carbon-Alginate Beads for Efficient Removal of Methylene Blue. *Int. J. Biol. Macromol. or Int. J. Biol. Macromol.* **2018**, *107*, 1792−1799.

(16) Metin, A. Ü.; Çiftçi, H.; Alver, E. Efficient Removal of Acidic Dye Using Low-Cost Biocomposite Beads. *Ind. Eng. Chem. Res.* **2013**, *52* (31), 10569−10581.

(17) Kurczewska, J.; Cegłowski, M.; Schroeder, G. Alginate/PAMAM Dendrimer−Halloysite Beads for Removal of Cationic and Anionic Dyes. *Int. J. Biol. Macromol. or Int. J. Biol. Macromol.* **2019**, *123*, 398−408.

(18) Pishdadi-Aghdarreh, F.; Norouzbeigi, R.; Velayi, E. Simultaneous Adsorption of Methylene Blue Cationic Dye and Paraquat Herbicide on Activated Lightweight Expanded Clay Aggregate (LECA) as a Sustainable and Recyclable Adsorbent. *Appl.Clay Sci.* **2024**, *256*, 107432.

(19) Zhang, Y.; Zhang, Y.; Luo, X.; Gao, Q.; Liu, Y.; Wang, X.; Zhou, S.; Wang, D.; Gu, P.; Li, Z. Superfast Removal of Dyes and Herbicides with Triphenylamine-Based Porous Organic Polymers by One-Step Sulfonation and Carboxylation. *Sep. Purif. Technol.* **2023**, *327*, 124799.

(20) Intisar, A.; Ramzan, A.; Hafeez, S.; Hussain, N.; Irfan, M.; Shakeel, N.; Gill, K. A.; Iqbal, A.; Janczarek, M.; Jesionowski, T. Adsorptive and Photocatalytic Degradation Potential of Porous Polymeric Materials for Removal of Pesticides, Pharmaceuticals, and Dyes-Based Emerging Contaminants from Water. *Chemosphere* **2023**, *336*, 139203.

(21) Sakthivel, R.; Palanisamy, P.; Selvaraj, S. K.; Baki, Z. A.; Vijayaraghavalu, S. S. Cu3(BTC)2 Metal Organic Framework as a Promising Adsorbent for Operative Exclusion of Toxic Dyes and Herbicide. *Results Mater.* **2024**, *21*, 100512.

(22) Gupta, V. K.; Rastogi, A. Biosorption of Lead from Aqueous Solutions by Green Algae Spirogyra Species: Kinetics and Equilibrium Studies. *J. Hazard. Mater.* **2008**, *152* (1), 407−414.

(23) Gupta, V. K.; Rastogi, A.; Nayak, A. Biosorption of Nickel onto Treated Alga (Oedogonium Hatei): Application of Isotherm and Kinetic Models. *J. Colloid Interface Sci.* **2010**, *342* (2), 533−539.

(24) Gupta, V. K.; Rastogi, A.; Nayak, A. Adsorption Studies on the Removal of Hexavalent Chromium from Aqueous Solution Using a Low Cost Fertilizer Industry Waste Material. *J. Colloid Interface Sci.* **2010**, *342* (1), 135−141.

(25) Gupta, V. K.; Jain, R.; Mittal, A.; Mathur, M.; Sikarwar, S. Photochemical Degradation of the Hazardous Dye Safranin-T Using TiO2 Catalyst. *J. Colloid Interface Sci.* **2007**, *309* (2), 464−469.

(26) Gupta, V. K.; Ali, I.; Saini, V. K. Adsorption Studies on the Removal of Vertigo Blue 49 and Orange DNA13 from Aqueous Solutions Using Carbon Slurry Developed from a Waste Material. *J. Colloid Interface Sci.* **2007**, *315* (1), 87−93.

(27) Gupta, V. K.; Mittal, A.; Gajbe, V.; Mittal, J. Removal and Recovery of the Hazardous Azo Dye Acid Orange 7 through Adsorption over Waste Materials: Bottom Ash and De-Oiled Soya. *Ind. Eng. Chem. Res.* **2006**, *45* (4), 1446−1453.

(28) Gupta, V. K.; Jain, R.; Malathi, S.; Nayak, A. Adsorption−Desorption Studies of Indigocarmine from Industrial Effluents by Using Deoiled Mustard and Its Comparison with Charcoal. *J. Colloid Interface Sci.* **2010**, *348* (2), 628−633.

(29) Gupta, V. K.; Jain, R.; Varshney, S. Removal of Reactofix Golden Yellow 3 RFN from Aqueous Solution Using Wheat Husk—An Agricultural Waste. *J. Hazard. Mater.* **2007**, *142* (1), 443−448.

(30) Gupta, V. K.; Ali, I. Removal of Endosulfan and Methoxychlor from Water on Carbon Slurry. *Environ. Sci. Technol.* **2008**, *42* (3), 766−770.

(31) Gupta, V. K.; Gupta, B.; Rastogi, A.; Agarwal, S.; Nayak, A. Pesticides Removal from Waste Water by Activated Carbon Prepared from Waste Rubber Tire. *Water Res.* **2011**, *45* (13), 4047−4055.

(32) Redding, A. M.; Cannon, F. S.; Snyder, S. A.; Vanderford, B. J. A QSAR-like Analysis of the Adsorption of Endocrine Disrupting Compounds, Pharmaceuticals, and Personal Care Products on Modified Activated Carbons. *Water Res.* **2009**, *43* (15), 3849−3861.

(33) Fito, J.; Abewaa, M.; Mengistu, A.; Angassa, K.; Ambaye, A. D.; Moyo, W.; Nkambule, T. Adsorption of Methylene Blue from Textile Industrial Wastewater Using Activated Carbon Developed from Rumex Abyssinicus Plant. *Sci. Rep* **2023**, *13* (1), 5427.

(34) Takele, T.; Angassa, K.; Abewaa, M.; Kebede, A. M.; Tessema, I. Adsorption of Methylene Blue from Textile Industrial Wastewater Using Activated Carbon Developed from H3PO4-Activated Khat Stem Waste. *Biomass Conv. Bioref.* **2025**, *15*, 4085.

(35) Yaqub, A.; Syed, S. M.; Ajab, H.; Zia Ul Haq, M. Activated Carbon Derived from *Dodonaea Viscosa* into Beads of Calcium-Alginate for the Sorption of Methylene Blue (MB): Kinetics, Equilibrium and Thermodynamics. *J. Environ. Manage.* **2023**, *327*, 116925.

(36) Vinayagam, R.; Ganga, S.; Murugesan, G.; Rangasamy, G.; Bhole, R.; Goveas, L. C.; Varadavenkatesan, T.; Dave, N.; Samanth, A.; Radhika Devi, V.; Selvaraj, R. 2,4-Dichlorophenoxyacetic Acid (2,4-D) Adsorptive Removal by Algal Magnetic Activated Carbon Nanocomposite. *Chemosphere* **2023**, *310*, 136883.

(37) Yazid, H.; Grich, A.; Bahsis, L.; Regti, A.; El Himri, M.; El Haddad, M. Exploring and Studying the Adsorption Mechanisms of the Herbicides 2,4,5-T and 2,4-D on Activated Carbon from *Walnut Shells*, Using Theoretical DFT Analyses and a Central Composite Design. *Results Surf. Interface* **2024**, *14*, 100192.

(38) Ozcan, D. O.; Hendekci, M. C.; Ovez, B. Enhancing the Adsorption Capacity of Organic and Inorganic Pollutants onto Impregnated Olive Stone Derived Activated Carbon. *Heliyon* **2024**, *10*, e32792.

(39) Aouaini, F.; Dhaouadi, F.; Georgin, J.; Stracke Pfingsten Franco, D.; Alyousef, H.; Bonilla-Petriciolet, A.; Ben Lamine, A. Statistical Physics Analysis of the Adsorption of Reactive Red 141 Dye on Residual Avocado Peel (*Persea Americana*) Chemically Modified with H2SO4 and HNO3. *Inorg. Chem. Commun.* **2024**, *165*, 112547.

(40) Sboui, N.; Sellaoui, L.; Dhaouadi, F.; Deng, S.; Bonilla-Petriciolet, A.; Boughzala, K. Advanced Analysis of the Adsorption Mechanism of Textile Pollutant on Britholites: Modelling via Statistical Physics. *CHEM AFR.* **2024**, *7*, 4411.

(41) Atri, A.; Dhaouadi, F.; Mechi, N.; Sellaoui, L.; Echabaane, M.; Ben Chaabane, R.; Erto, A.; Badawi, M.; Ben Lamine, A. Removal of Textile Pollutants from Aqueous Medium Using Biosynthesized CuO Nanoparticles: Theoretical Comparative Investigation via Analytical Model. *Heliyon* **2024**, *10* (5), e26285.

(42) Vener, M. V.; Makhrov, D. E.; Voronin, A. P.; Shalafan, D. R. Molecular Dynamics Simulation of Association Processes in Aqueous Solutions of Maleate Salts of Drug-like Compounds: The Role of Counterion. *Int. J. Mol. Sci.* **2022**, *23* (11), 6302.

(43) Dhaouadi, F.; Aouaini, F.; Basha, B.; Bonilla-Petriciolet, A.; Georgin, J.; Ben Lamine, A. Evaluation and Analysis of the Adsorption Mechanism of Three Emerging Pharmaceutical Pollutants on a Phosphorised Carbon-Based Adsorbent: Application of Advanced Analytical Models to Overcome the Limitation of Classical Models. *Heliyon* **2024**, *10* (14), e34788.

(44) Aouaini, F.; Dhaouadi, F.; Georgin, J.; Franco, D. S. P.; Alyousef, H.; Erto, A.; Lamine, A. B. Application of Physical Statistical Modeling in the Adsorption of the Drug Ketoprofen and the 2,4-D Herbicide Using the Bark Campomanesia Guazumifolia Forest Species Modified with H2SO4 as an Adsorbent. *Adv. Theory Simul.* **2024**, 7, 2400236.

(45) Dhaouadi, F.; Sellaoui, L.; Taamalli, S.; Louis, F.; El Bakali, A.; Badawi, M.; Georgin, J.; Franco, D. S.P.; Silva, L. F.O.; Bonilla-Petriciolet, A.; Rtimi, S. Enhanced Adsorption of Ketoprofen and 2,4-Dichlorophenoxyactic Acid on Physalis Peruviana Fruit Residue Functionalized with H2SO4: Adsorption Properties and Statistical Physics Modeling. *Chem. Eng. J.* **2022**, *445*, 136773.